 CMES, vol.5, no.1, pp.5-20, 2004

Multi-Inclusion Unit Cell Studies of Reinforcement Stresses and Particle Failure in Discontinuously Reinforced Ductile Matrix Composites

H.J. Böhm[1], W. Han[1,2] and A. Eckschlager[1,3]

Abstract: Three-dimensional periodic micromechanical models are used for studying the mechanical behavior of discontinuously reinforced ductile matrix composites. The models are based on unit cells that contain a number of randomly positioned and, where applicable, randomly oriented spherical, spheroidal or cylindrical reinforcements. The Finite Element method is used to resolve the microscale stress and strain fields and to predict the homogenized responses under overall uniaxial tensile loading in the elastic and elastoplastic regimes. Periodicity boundary conditions are employed in the analyses. The main emphasis of the contribution is put on studying the microscale stresses in the reinforcements, which are evaluated in terms of both phase averages and "inclusion averages". The dependence of the inclusion averaged stresses on the fiber orientation is discussed for composites reinforced by randomly oriented short fibers, good agreement being found between unit cell and mean field models. For the case of spherical reinforcements the stresses in the particles are used to trigger brittle cleavage via a Weibull fracture criterion. The probabilistic algorithm can be used to model consecutive particle fracture in particle reinforced ductile matrix composites.

keyword: Continuum micromechanics, unit cells, MMCs, particle cleavage.

1 Introduction

Discontinuously reinforced ductile matrix composites, such as particle and short fiber reinforced metal matrix composites (MMCs), are materials of considerable technological importance. They aim at combining desirable properties of a metallic matrix, especially its ductility, and of the reinforcements, such as high stiffness, hardness and abrasion resistance. Consequently, the mechanical behavior of ductile matrix composites differs from that of monolithic metals in several important aspects and has been the subject of considerable research interest for the past 25 years.

A natural starting point for modeling the mechanical behavior of composites consists in explicitly accounting for their heterogeneity at a length scale where matrix and reinforcements are clearly distinguishable, which is called the microscale in the following. This philosophy forms the basis of continuum micromechanics of materials, a research field in which two main modeling strategies have been developed since the 1960s. One of them employs homogeneous comparison materials and statistical information on the microscale geometry of the composite to obtain estimates for and bounds on the overall thermomechanical responses of elastic and inelastic composites. The most important approaches of this type are mean field and Hashin–Shtrikman-type variational theories; a recent overview of such methods was given by Ponte Castañeda and Suquet (1998). Alternatively, simplified "model composites" may be studied, which in most cases take the form of periodic phase arrangements described via appropriate unit cells that are analyzed at a high level of detail by numerical engineering methods. The latter group of "discrete microstructure" models are the main tool used in the present work.

An improved understanding of the thermomechanical behavior of composites reinforced by aligned short fibers has been the aim of considerable research efforts, studies based on axisymmetric cell models, see e.g. Christman, Needleman, and Suresh (1989) and Tvergaard (1990), on three-dimensional single-fiber unit cells, see e.g. Levy and Papazian (1990), and on three-dimensional multi-fiber unit cells, see Ingber and Papathanasiou (1997) and Gusev, Lusti, and Hine (2002), having been published. In contrast, only a small number of discrete microstructure models have been reported that address composites rein-

[1] Christian Doppler Laboratory for Functionally Oriented Materials Design, Institute of Light Weight Structures and Aerospace Engineering, Vienna University of Technology, Vienna, Austria.
[2] now with Stadler Altenrhein AG, Switzerland.
[3] now with Neusiedler AG, Ulmerfeld–Hausmening, Austria.

forced by nonaligned short fibers. Planar Finite Element based models were developed by Courage and Schreurs (1992), a three-dimensional description of alternatingly tilted fibers was proposed by Sørensen, Suresh, Tvergaard, and Needleman (1995), and multi-fiber unit cells in combination with the Boundary Element method were reported by a number of groups, among them Banerjee and Henry (1992), and Ingber, Womble, and Mondy (1992). Like a recent Finite Element study of nonaligned short fiber reinforced composites by Lusti, Hine, and Gusev (2002) the latter models were restricted to elastic constituent behavior and low fiber volume fractions. Three-dimensional unit cell models of ductile matrix composites with randomly oriented fibers at nondilute volume fractions, compare Böhm, Eckschlager, and Han (2002), are a very recent development.

With regard to particle reinforced composites, a large body of literature involving discrete microstructure models has been reported since the 1970s. Published unit cell studies have involved widely differing levels of geometrical complexity, ranging from square arrays of spheres, see e.g. Agarwal and Broutman (1974), and different types of axisymmetric models, see e.g. Agarwal, Panizza, and Broutman (1971) and Weissenbek, Böhm, and Rammerstorfer (1994), to periodic arrangements of cells containing a considerable number of randomly positioned inhomogeneities. The latter approach was first employed with two-dimensional unit cell models, which have reached an impressive level of development, compare e.g. Lee, Moorthy, and Ghosh (1999). Three-dimensional multi-particle unit cell models have been extended from studying the elastic response of particle reinforced composites, see e.g. Gusev (1997), to research concentrating on the elastoplastic behavior of ductile matrix composites, see Böhm, Eckschlager, and Han (1999) and Segurado, LLorca, and González (2002). Recent studies by Böhm and Han (2001) as well as Shen and Lissenden (2002) showed that three-dimensional models of the above type are much better suited to describing particle reinforced composites than are planar models.

On the microscale, damage and failure of ductile matrix composites can be attributed to three mechanisms, viz. ductile failure of the matrix, decohesion of the interface between reinforcements and matrix, and brittle cleavage of the reinforcements. The relative importance of these three damage modes varies widely among different composites and depends to a large extent on the material behavior of the constituents and on the size of the reinforcements. Various modeling approaches have been reported for studying each of the above microscopic damage modes and there is continuing intensive research interest in these problems. For the brittle failure of discontinuous reinforcements embedded in a ductile matrix, which is of special relevance for the present study, published models have involved pre-cracked particles, see e.g. Bao (1992), cohesive surface descriptions of cracks progressing through a reinforcement, see e.g. Tvergaard (1993), "element death" algorithms for crack growth, see e.g. Mishnaevsky, Lippmann, and Schmauder (2001), and models based on "instantaneous" cleavage of particles along predefined fracture planes triggered by deterministic (Rankine-type) or statistical (Weibull-type) criteria, see e.g. Pandorf (2000). In most simulations particle cleavage was assumed to take place at some symmetry plane of the model geometry, among the exceptions being some multi-inclusion unit cell models employing planar phase arrangements, such as those of Ghosh and Moorthy (1998) or Berns, Melander, Weichert, Asnafi, Broeckmann, and Gross-Weege (1998), as well as two-dimensional embedded cell models for studying macrocracks in particle reinforced materials as reported by Mishnaevsky, Lippmann, and Schmauder (2001).

The present contribution focuses on the use of three-dimensional multi-inclusion unit cell models for studying two issues that are of considerable interest in understanding the mechanical behavior of discontinuously reinforced materials. One of them is the dependence on the fiber orientation of the stress fields in randomly oriented reinforcing fibers, and the other involves the modeling of the accumulation of microscale damage due to the consecutive brittle cleavage of spherical particles embedded in a ductile matrix.

2 Modeling Considerations

In the simplest case the modeling of the mechanical behavior of composite materials by multi-inclusion unit cells requires three main steps: the generation and meshing of appropriate phase arrangements, the evaluation of the microscale stresses and strains in the unit cell, and the processing of the results in terms of the overall (homogenized) material behavior or appropriate graphical representations and/or numerical descriptors of the microfields.

For the present study the particle or fiber positions within

each unit cell were generated via a Random Sequential Adsorption algorithm, in which a new randomly positioned (and, where applicable, randomly oriented) reinforcement is retained if it maintains a user selected minimum distance to all previously accepted inclusions and is rejected otherwise. In addition, periodicity of the arrangement of the reinforcements within the unit cells was enforced, as is evident in fig.1. This method is suitable for generating statistically uniform arrangements of particles and fibers at low to moderate volume fractions. At higher reinforcement volume fraction geometrical frustration tends to set in due to a dearth of suitable unoccupied volumes for positioning additional inclusions. For such geometries more sophisticated methods must be used, which may be based, for example, on Monte Carlo procedures as reported by Gusev, Hine, and Ward (2000), on simulated annealing algorithms as introduced by Rintoul and Torquato (1997), or on genetic algorithms, compare Zeman and Šejnoha (2001).

The present study employs unit cells that contain some 15 randomly positioned identical spheres for modeling particle reinforced composites (PRCs) or 15 randomly positioned and oriented identical spheroidal or cylindrical fibers for describing random short fiber reinforced composites (RSFRCs). For the latter type of microgeometries phase arrangements were generated such that spheroidal or cylindrical fibers can occupy the same positions and have the same orientations in order to allow a direct assessment of fiber shape effects. Representatives of the above three types of periodic unit cells are depicted in fig.1.

The unit cells were meshed with 10-node tetrahedral elements using the preprocessor PATRAN V.8.5 (MacNeal–Schwendler Corp., Los Angeles, CA), compatible meshes at opposite faces of the unit cells being enforced. Typical element counts were of the order of 100000. Due to difficulties in meshing certain geometrical details it was found to be necessary to reject configurations containing reinforcements that very closely approach cell boundaries or fibers that intersect cell faces at very small angles. The elastic singularities that may occur at the sharp edges of cylindrical fibers were not fully resolved, auxiliary axisymmetric models being used to check that the mesh sizes were sufficiently fine for accounting for the edges' influence on the averages of the microscale stresses and strains.

The elastic and elastoplastic responses of the unit cells

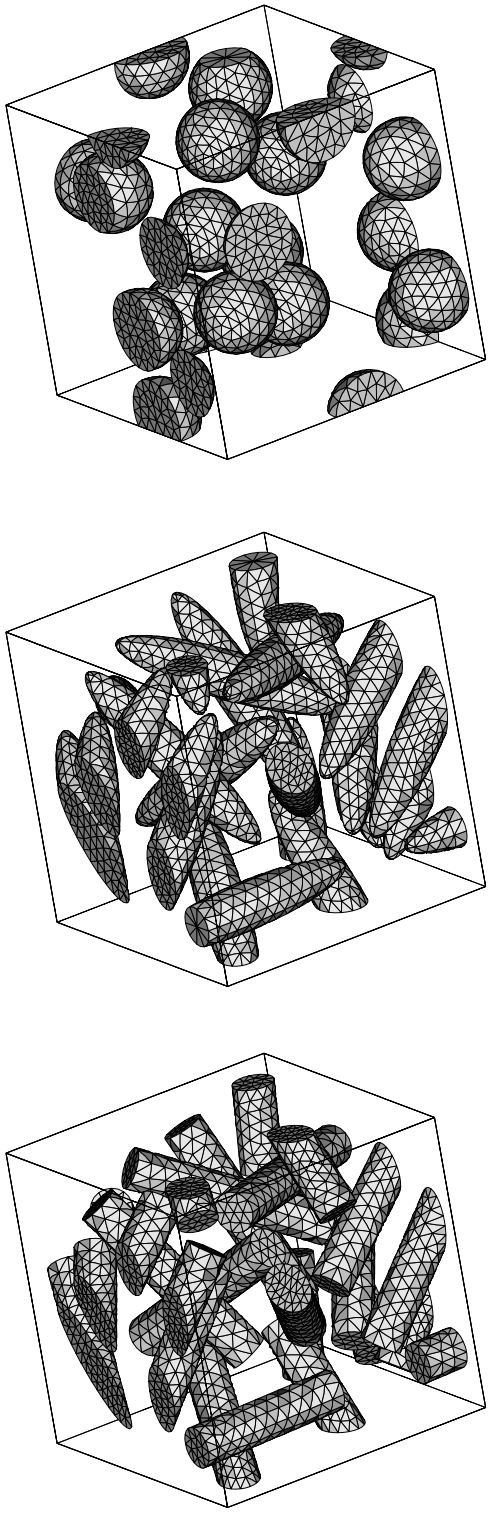

Figure 1 : Periodic unit cells containing 15 spherical particles (top), 15 randomly oriented spheroidal fibers (center), and 15 randomly oriented cylindrical fibers (bottom) at a volume fraction of ξ=0.15.

under uniaxial tensile loading were evaluated with the commercial Finite Element program ABAQUS/Standard V.5.8 (Hibbitt, Karlsson and Sorensen Inc., Pawtucket, RI), geometrically nonlinear analyses being employed. The periodicity boundary conditions were enforced via multi-point constraints that link the displacement vectors $\mathbf{u}$ of the i-th pair of nodes that lie on opposite faces of a unit cell via relations of the type

$$\mathbf{u}(\mathbf{r}_{i,2}) = \mathbf{u}(\mathbf{r}_{i,1}) + \Delta\mathbf{u}_{12} \quad . \tag{1}$$

Here $\mathbf{r}_{i,1}$ and $\mathbf{r}_{i,2}$ stand for the coordinate vectors of the pair of nodes and $\Delta\mathbf{u}_{12}$ describes the difference in displacement between the two opposite faces, 1 and 2, as obtained from the displacements of appropriately positioned "master nodes".

Such periodicity boundary conditions can be used with both displacement and load controlled analyses and they provide unique estimates for the overall mechanical behavior of the underlying phase arrangements that lie between the lower and upper bounds which can be obtained with homogeneous stress and strain boundary conditions, respectively, see e.g. Suquet (1987). Specially developed algorithms described in section 3.2 were used for modeling the brittle cleavage of reinforcing particles.

It may be noted at this point that higher computational efficiency may be reached in unit cell studies by using Finite Element codes that are specifically geared to micromechanical analyses, see e.g. Ghosh and Moorthy (1998) or Zohdi and Wriggers (2001), although there may be a price to be paid in terms of geometrical flexibility. Furthermore, other numerical engineering methods may be employed to advantage in discrete microstructure models of inhomogeneous materials, studies using the Boundary Element method (as mentioned in section 1), Fast Fourier Transforms, compare Michel, Moulinec, and Suquet (2000), equivalent inclusion methods, compare Fond, Riccardi, Schirrer, and Montheillet (2001), and spring networks, compare Ostoja-Starzewski (1998), having been reported.

The evaluation of the results obtained from three-dimensional multi-inclusion unit cells has proven rather complex. Visualization of the microscale stress and strain fields can take the form of color coded fringes on the unit cell's surface, on the reinforcements' surfaces, and on planar sections through the unit cells as used e.g. in Böhm, Eckschlager, and Han (2002), or of iso-surfaces within the unit cell. Neither of these approaches reliably provides "intuitive" representations of the microfields, especially of those in the matrix.

Alternatively, numerical descriptors may be used for assessing the microfields. The simplest of them are phase averages of the microscale stresses and strains, which have the advantage of allowing direct comparisons with results from mean field methods. ABAQUS provides options for accessing the volume corresponding to each integration point, so that the phase average of some function f can be approximated as

$$\overline{f} = \frac{1}{V^{(j)}} \int_{V^{(j)}} f(\mathbf{r}) dV \approx \frac{1}{V^{(j)}} \sum_{l=1}^{N^{(j)}} f_l V_l \quad . \tag{2}$$

Here, f_l and V_l are the function value and the integration weight (in terms of an integration point volume), respectively, associated with the l-th integration point within a given phase (j), which contains $N^{(j)}$ integration points and has a phase volume $V^{(j)}$. Equation (2) can easily be extended to evaluating higher statistical moments of f.

Phase averages and the corresponding phase-level standard deviations, however, are not particularly sensitive instruments for probing arrangement specific variations in the distributions of the microscale stresses and strains. For composites with matrix–inclusion topology, considerably more detailed information can be extracted by evaluating the averages and standard deviations of the microfields within individual reinforcements, which can be obtained by interpreting $N^{(j)}$ and $V^{(j)}$ in eqn. (2) as pertaining to single particle or fiber rather than to the collective of all reinforcements. This concept of "inclusion averages" plays an important role in the discussion of the stresses present in randomly oriented short fibers given in section 3.1 and is closely related to the evaluation of Weibull fracture probabilities at the particle level employed in section 3.2.

The use of multi-inclusion unit cells immediately gives rise to the question of how many reinforcements are required for describing the mechanical behavior of a given composite with satisfactory realism and accuracy, the optimum case being a unit cell that is a proper reference volume element as defined e.g. by Hashin (1983). For the special case of statistically isotropic elastic composites reinforced by spherical particles Drugan and Willis (1996) provided estimates that correlate the error in the overall elastic moduli with the linear dimensions of (non-periodic) evaluation volumes. Excellent agreement with their results, which imply that reasonable predictions for

the homogenized elastic behavior of such materials can be obtained from rather small unit cells, has been reported by Gusev (1997), Michel, Moulinec, and Suquet (1999), Segurado and LLorca (2002), Böhm and Han (2001), as well as Han, Eckschlager, and Böhm (2001). The latter two studies also showed that unit cells containing some 15 to 20 spherical particles give predictions for the elastic phase averaged microstresses that closely approach mean field results.

No comparable considerations are available for more general phase arrangements (such as nonaligned fibers) or for inelastic composites, although the "windowing methods" discussed by Jiang, Ostoja-Starzewski, and Jasiuk (2000) in principle allow to assess how closely a given configuration approaches a proper reference volume element. Segurado, LLorca, and González (2002) recently reported good agreement between the elastoplastic uniaxial tensile response of a unit cell containing some 30 randomly positioned spherical particles and results of the modified secant scheme of Suquet (1995). There are, however, strong indications that for elastoplastic matrix behavior much larger unit cells may be required than for elastic response, see e.g. Böhm and Han (2001) and Jiang, Ostoja-Starzewski, and Jasiuk (2000), especially in the case of matrix materials showing weak or no strain hardening. This is thought to be due to the inhomogeneous distribution of the plastic strains in the matrix, which effectively lead to the formation of inhomogeneous regions that become considerably larger than typical particle distances with increasing plastic strains.

3 Discussion of results

All results given in the present contribution refer to the same combination of constituents, SiC reinforcements in an Al2618-T4 matrix, for which damage by reinforcement fracture plays an important role, compare LLorca, Martín, Ruiz, and Elices (1993). The elastoplastic material behavior of the aluminum matrix was described by J_2-plasticity, isotropic hardening following a modified Ludwik hardening law being used. A linear elastic description was employed for the SiC reinforcements and a perfectly strong interface between reinforcements and matrix was prescribed. The material parameters used for the constituents are listed in table 1, where E stands for the Young's modulus, ν for the Poisson ratio, $\sigma_{y,0}$ for the initial yield stress, h for the hardening parameter, n for the hardening exponent, and σ_f for the tensile strength of the fibers and particles. All unit cells correspond to a nominal reinforcement volume fraction of ξ=0.15.

3.1 Composites reinforced by randomly oriented short fibers

The results presented in this section refer to damage free MMCs consisting of an Al2618-T4 matrix reinforced by SiC particles or by randomly oriented SiC fibers of aspect ratio a=5.0. For the material parameters used, compare table 1, the critical fiber aspect ratio $a_c = \sigma_f / 2\tau_y^{(m)}$ evaluates as approximately 4, so that the above reinforcements can be viewed as fully fledged short fibers.

3.1.1 Elastic response

Table 2 lists a number of analytical and numerical predictions for the homogenized Young's modulus E^* and Poisson ratio ν^* of SiC/Al composites reinforced by 15 vol.% of spherical particles or randomly oriented short fibers. The Hashin–Shtrikman bounds (Hashin and Shtrikman (1962), denoted as HSB) hold for any overall isotropic two-phase material and thus are applicable to both types of composites considered here. The three-point bounds (PRC/3PB) for materials reinforced by non-interpenetrating spheres of identical size, compare Torquato (1991), and estimates obtained with the generalized self consistent scheme (PRC/GSCS) of Christensen and Lo (1979) can be directly compared to the results from unit cells containing randomly positioned spherical particles (PRC/sp). For the MMCs reinforced by randomly oriented short fibers, Mori–Tanaka estimates (RSFRC/MTM) evaluated according to Benveniste (1987) are listed in addition to unit cell predictions for spheroidal (RSFRC/sph) and cylindrical (RSFRC/cyl) fibers. The unit cell results given in this and the subsequent tables are ensemble averages obtained from a number of runs.

All unit cell predictions for E^* can be seen to lie within the Hashin–Shtrikman bounds and to be fairly close to the lower bound, which is to be expected for materials consisting of stiffer inhomogeneities embedded in a softer matrix, compare Torquato (1991). The results obtained for spherical particles, (PRC/sp), also fulfill the appropriate three-point bounds. Composites reinforced by randomly oriented short fibers can be seen to show a small but noticeable increase in the overall Young's modulus compared to materials reinforced by spherical particles even at the moderate elastic contrast of 6.43.

Table 1 : Material parameters used for the elastoplastic Al2618–T4 matrix (modified Ludwik hardening law) and the elastic SiC reinforcements.

	E [GPa]	ν [ ]	$\sigma_{y,0}$ [MPa]	h [MPa]	n [ ]	σ_f [GPa]
Al2618	70	0.30	184	722.7	0.49	—
SiC	450	0.17	—	—	—	1.0

Table 2 : Analytical and numerical predictions for the overall elastic moduli of isotropic particle and short fiber (a=5.0) reinforced SiC/Al2618 MMCs (ξ=0.15).

	E^* [GPa]	ν^* [ ]
HSB	87.6–106.1	0.246–0.305
PRC/3PB	87.9–89.2	0.283–0.287
PRC/GSCS	87.8	0.286
PRC/sp	87.9	0.286
RSFRC/MTM	89.8	0.285
RSFRC/sph	89.4	0.285
RSFRC/cyl	90.0	0.284

Table 3 : Analytical and numerical predictions for the phase averaged normalized elastic microstresses in SiC/Al2618 MMCs (ξ=0.15) reinforced by particles and randomly oriented short fibers (a=5.0) under uniaxial tensile loading.

	$\overline{\sigma}^{(m)}_{eqv}$ [ ]	$\overline{\sigma}^{(m)}_{m}$ [ ]	$\overline{\sigma}^{(r)}_{eqv}$ [ ]	$\overline{\sigma}^{(r)}_{m}$ [ ]
PRC/MTM	0.89	0.31	1.62	0.44
PRC/GSCS	0.89	0.31	1.64	0.44
PRC/sp	0.90	0.31	1.69	0.44
	$\pm$0.16	$\pm$0.11	$\pm$0.20	$\pm$0.08
RSFRC/MTM	0.86	0.31	1.78	0.49
RSFRC/sph	0.89	0.31	1.86	0.48
	$\pm$0.16	$\pm$0.09	$\pm$0.46	$\pm$0.26
RSFRC/cyl	0.88	0.31	1.92	0.49
	$\pm$0.15	$\pm$0.09	$\pm$0.52	$\pm$0.29

In order to allow some assessment of the microfields, predictions for the phase averages of the von Mises equivalent stress σ_{eqv} and of the mean stress σ_m in matrix (m) and reinforcements (r) are listed in table 3 for uniaxial tensile loading. The stresses are normalized with respect to the applied load, so that they can be interpreted in terms of phase concentration factors. For the unit cell results the phase-level standard deviations are also given. There is surprisingly little difference in both the phase averages and the standard deviations of the matrix stresses obtained for composites reinforced by particles and by random short fibers, with only a very small reduction of the stress level in the matrix being evident for the latter case. In contrast, the phase averages of the equivalent stresses in the fibers are significantly higher than those in the particles, a smaller effect being present for the mean stresses.

Table 3 also shows clearly that the phase-level standard deviations of $\sigma^{(r)}_{eqv}$ and $\sigma^{(r)}_{m}$ are much higher for the random fiber composite, which must be a consequence of stronger inter-inclusion and/or intra-inclusion stress fluctuations in the fibers compared to the spherical particles. Further light can be shed on this issue by evaluating the inclusion averages of the microstresses together with the corresponding standard deviations, i.e. by studying the microfields in individual fibers or particles. The inclusion averages of the equivalent stress in the particles were found to range between approximately 85% and 125% of the phase average, whereas for both types of short fiber reinforcement considered here the range is 75% to 180%. The corresponding values for the mean stress are 75% to 140% (PRC) and 35% to 230% (RSFRC). As expected, the variation of the averaged microstresses between individual reinforcements thus tends to be significantly larger in overall isotropic composites containing randomly oriented short fibers than in materials reinforced by particles.

The above assessment indicates that it may be worth-

while to adapt mean field theories (which generally are effective in capturing aspect ratio effects) for extracting information on microfields in dependence on the orientation of reinforcements. This can, in fact, be achieved by interpreting the central equation in the formulation of the Mori–Tanaka method due to Benveniste (1987) in terms of the average stresses in fibers of a given orientation (i.e. the equivalent of inclusion averages) rather than phase averages. The (nondilute) Mori-Tanaka stress concentration tensor for fibers having some given orientation, $\overline{\mathbf{B}}_{\mathrm{MT}}^{(\mathrm{r})\angle}$, is then given by

$$\overline{\mathbf{B}}_{\mathrm{MT}}^{(\mathrm{r})\angle} = \overline{\mathbf{B}}_{\mathrm{dil}}^{(\mathrm{r})\angle}\ \overline{\mathbf{B}}_{\mathrm{MT}}^{(\mathrm{m})} \quad , \tag{3}$$

where $\overline{\mathbf{B}}_{\mathrm{MT}}^{(\mathrm{m})}$ stands for the phase averaged Mori–Tanaka matrix stress concentration tensor and $\overline{\mathbf{B}}_{\mathrm{dil}}^{(\mathrm{r})\angle}$ denotes the dilute stress concentration tensor transformed from the fiber coordinate system to the global coordinate system. The orientation dependent average stress tensors in the fibers can then be extracted as

$$\overline{\sigma}^{(\mathrm{r})\angle} = \overline{\mathbf{B}}_{\mathrm{MT}}^{(\mathrm{r})\angle}\ \overline{\sigma} \quad , \tag{4}$$

for any applied macroscopic stress field $\overline{\sigma}$. For more detailed discussions of the approach see Duschlbauer, Pettermann, and Böhm (2003).

The evaluation of $\overline{\mathbf{B}}_{\mathrm{dil}}^{(\mathrm{r})\angle}$ is straightforward and $\overline{\mathbf{B}}_{\mathrm{MT}}^{(\mathrm{m})}$ can be obtained from "multi-phase" Mori–Tanaka methods that were developed for describing composites with nonaligned reinforcements e.g. by Dunn, Ledbetter, Heyliger, and Choi (1996), by Pettermann, Böhm, and Rammerstorfer (1997), and by Mlekusch (1998). While being easy to handle and capable of producing useful results for many applications such multi-phase Mori–Tanaka models are of an ad-hoc nature and can give rise to non-symmetric "elastic tensors" under certain conditions, compare e.g. Benveniste (1990), Ferrari (1991), and Schjødt-Thomsen and Pyrz (2001). This is due to the fact that Mori–Tanaka methods are intrinsically based on aligned ellipsoidal arrangements of inhomogeneities, see Ponte Castañeda and Willis (1995). It was noted by Schjødt-Thomsen and Pyrz (2001), however, that the above difficulties do not occur for two-phase materials with a randomly oriented fibrous reinforcement phase.

For composites reinforced by randomly oriented fibers subjected to uniaxial tensile loading the stresses in the individual fibers obtained via eqn. (4) can be plotted as functions of the angle subtended between a given fiber and the applied load. Figures 2 and 3 show such diagrams for the von Mises equivalent stress and the mean stress, respectively, predicted for the fibers in SiC/Al MMCs. In both figures, the unit cell results are presented, on the one hand, in the form of inclusion averages (UC/INCL) for a number of individual fibers (solid circles), the standard deviations of the stress distributions within the fibers being indicated by error bars, which directly indicate the magnitude of the intra-fiber stress fluctuations. On the other hand, the phase averages of the stresses in the reinforcements and the corresponding phase-wise standard deviations are given as horizontal lines designated as "UC/PH mean" and "UC/PH stdv", respectively. The Mori–Tanaka results for the angular dependence of the stress measures evaluated from eqn. (4) are shown as bold dotted lines marked as MTM. Unit cell predictions pertaining to spheroidal fibers (top) and cylindrical fibers (bottom) are displayed in both figures; the Mori–Tanaka results, of course, pertain to spheroids in both cases.

Very satisfactory agreement between numerical and analytical predictions for the angular variation of the inclusion averages is evident for both deviatoric and mean stresses, especially for the spheroidal fibers. This strongly supports the validity of both the unit cell and the mean field results in view of the very different approximations involved in the two approaches. As in the case of spherical particles, unit cells containing a rather low number of randomly oriented fibers evidently give useful results for the overall and local elastic responses.

The main contributions to inter-fiber stress fluctuations can be seen to be due to the fiber orientation. Nevertheless, noticeable differences are evident in the averages of the stresses acting in individual fibers that subtend similar angles to the applied load, i.e. fiber–fiber interactions also contribute to inter-fiber fluctuations. A comparison of figs. 2 and 3 shows that the reinforcement shape plays only a limited role in determining the average fiber stresses in the elastic range (compare also Hill's modification theorem as discussed e.g. by Huet, Navi, and Roelfstra (1991)). In contrast, the intra-fiber fluctuations of the microstresses are much more marked for cylindrical than for spheroidal fibers, even when both occupy the same position and have the same orientation. Despite the fairly low reinforcement volume fraction and elastic contrast of the composite studied here, the microfields in the fibers do not even approach the classical result for di-

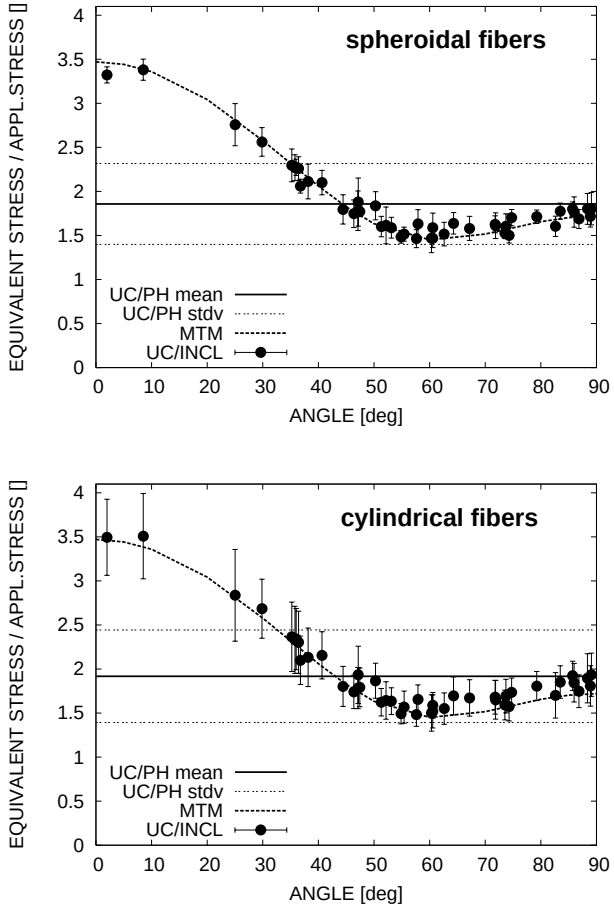

Figure 2 : Normalized equivalent stresses in the fibers as functions of the angle between the fibers and an applied uniaxial load $\overline{\sigma}$ in the elastic range; results comprise unit cell predictions for a SiC/Al2618 MMC reinforced by randomly oriented spheroidal (top) or cylindrical (bottom) fibers (a=5.0, ξ=0.15) and Mori–Tanaka mean field estimates (MTM).

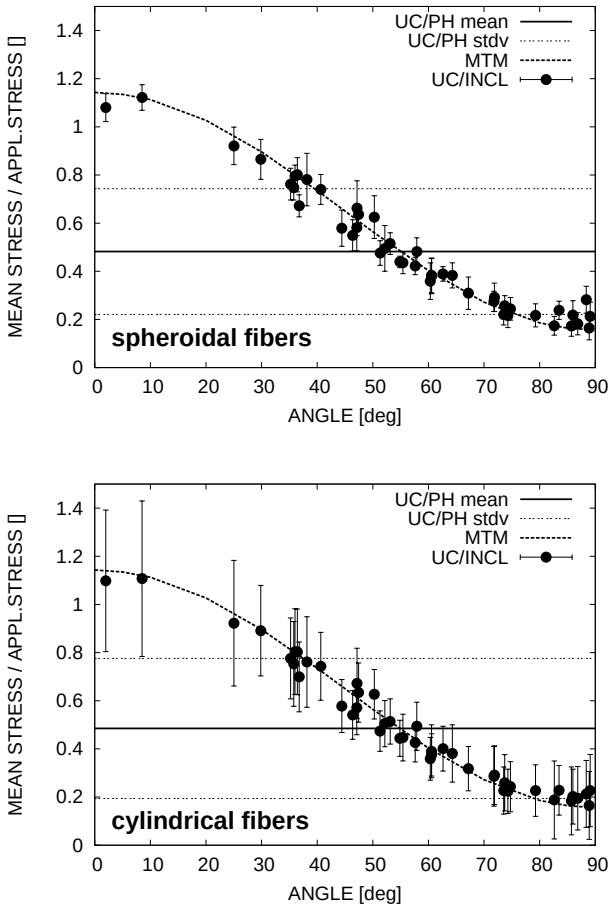

Figure 3 : Normalized mean stresses in the fibers as functions of the angle between the fibers and an applied uniaxial load $\overline{\sigma}$ in the elastic range; results comprise unit cell predictions for a SiC/Al2618 MMC reinforced by randomly oriented spheroidal (top) or cylindrical (bottom) fibers (a=5.0, ξ=0.15) and Mori–Tanaka mean field estimates (MTM).

lute composites due to Eshelby (1957), which states that intra-inclusion stress and strain fluctuations are zero for non-interacting ellipsoidal reinforcements.

Elevated stress levels are evident for fibers that are oriented at small angles with respect to the uniaxial load. In such fibers both the equivalent and the mean stresses markedly exceed both the corresponding phase averages and the even lower phase averages predicted for particle reinforced composites, compare table 3. This clearly shows the validity of a claim made earlier, viz. that phase averages and phase-wise standard deviations provide only very limited information on the microfields in nonaligned non-spherical reinforcements — they obviously cannot account for a situations where essentially a limited percentage of the reinforcements carry a large fraction of the applied load.

3.1.2 Elastoplastic response

For studying the behavior of MMCs reinforced by randomly oriented short fibers in the elastoplastic regime uniaxial tensile loading up to an applied stress of $\overline{\sigma}$ = 450 MPa, which corresponds to approximately 2.45 times the initial yield stress of the matrix, $\sigma_{y,0}^{(m)}$, was simulated. At

this load level the matrix can be viewed as having yielded throughout the composite.

Unit cell predictions for the phase averages of the accumulated equivalent plastic strain $\overline{\varepsilon}^{(m)}_{eqv,pl}$ and the von Mises stress $\overline{\sigma}_{eqv}$ in the matrix are listed in table 4 together with results for the equivalent and mean stresses in the reinforcements. In analogy to table 3 reinforcements in the form of randomly positioned spheres and of randomly positioned and oriented short fibers of spheroidal and cylindrical shape and aspect ratio a=5.0 are compared. Again all stresses are normalized to the applied stress.

Table 4 : Numerical predictions for the phase averaged normalized elastoplastic microstresses and microstrains in SiC/Al2618 MMCs (ξ=0.15, $\overline{\sigma}$=2.45$\sigma^{(m)}_{y,0}$) reinforced by particles and randomly oriented short fibers (a=5.0) under uniaxial tensile loading.

	$\overline{\varepsilon}^{(m)}_{eqv,pl}$ [$\times 10^{-2}$]	$\overline{\sigma}^{(m)}_{eqv}$ [ ]	$\overline{\sigma}^{(r)}_{eqv}$ [ ]	$\overline{\sigma}^{(r)}_{m}$ [ ]
PRC/sp	12.8	0.99	2.38	0.28
	$\pm$4.4	$\pm$0.09	$\pm$0.63	$\pm$0.28
RSFRC/sph	10.5	0.93	3.32	0.32
	$\pm$4.5	$\pm$0.10	$\pm$1.29	$\pm$0.74
RSFRC/cyl	8.4	0.88	3.50	0.30
	$\pm$3.8	$\pm$0.10	$\pm$1.73	$\pm$1.00

The accumulated plastic strain in the matrix is predicted to be highest for materials reinforced by spherical particles and about 35% lower for composites reinforced by randomly oriented cylinders, with the behavior of arrangement RSFRC/sph (randomly oriented spheroids) occupying an intermediate position. This allows the conclusion that for a given constituent behavior and for a given phase volume fraction randomly oriented fibers tend to give rise to noticeably stronger overall strain hardening compared to spherical particles in MMCs (it is interesting to note that preliminary studies by the authors have indicated that randomly oriented cube-shaped particles induce an increase in hardening nearly comparable to that caused by randomly oriented fibers). The phase averaged equivalent stresses in the reinforcements are predicted to be approximately 50% higher in the fiber reinforced materials, and the phase-level standard deviations of both equivalent and mean stresses are much higher than in the sphere filled composite.

Figure 4 displays the predicted orientational variation of the normalized von Mises equivalent stress in the reinforcements for both spheroidal and cylindrical fibers, and fig. 5 presents analogous data for the mean stress. As in figs. 2 and 3 the average stresses in individual fibers are marked by solid circles, the standard deviations of the corresponding stress distributions are represented by error bars, and the phase averages and phase-level standard deviations are indicated by horizontal lines.

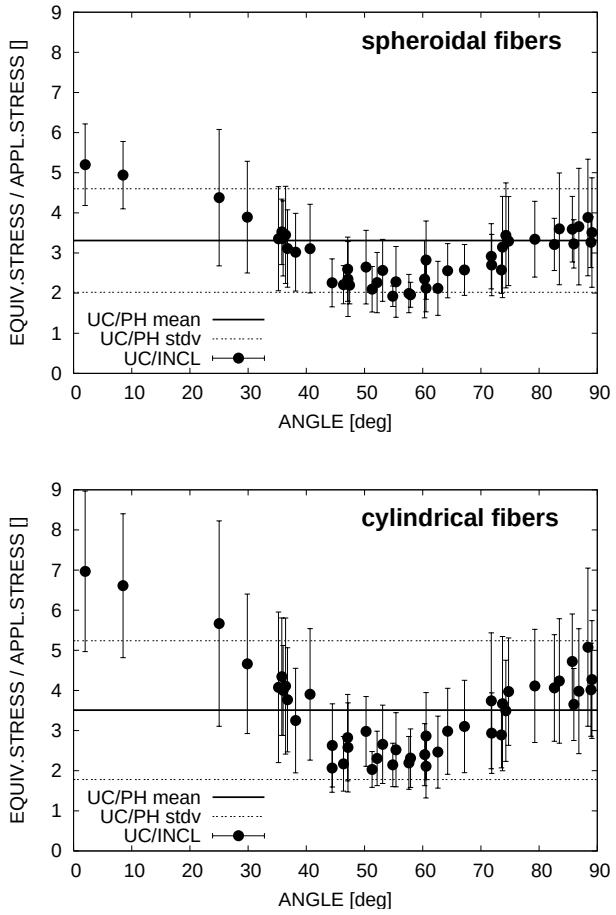

Figure 4 : Normalized equivalent stresses in the fibers as functions of the angle between the fibers and an applied uniaxial load $\overline{\sigma}$ in the fully yielded regime; results comprise unit cell predictions for an elastoplastic SiC/Al2618 MMC reinforced by randomly oriented spheroidal (top) or cylindrical (bottom) fibers (a=5.0, ξ=0.15, $\overline{\sigma}$=2.45$\sigma^{(m)}_{y,0}$).

Compared to the predictions for the elastic range, see

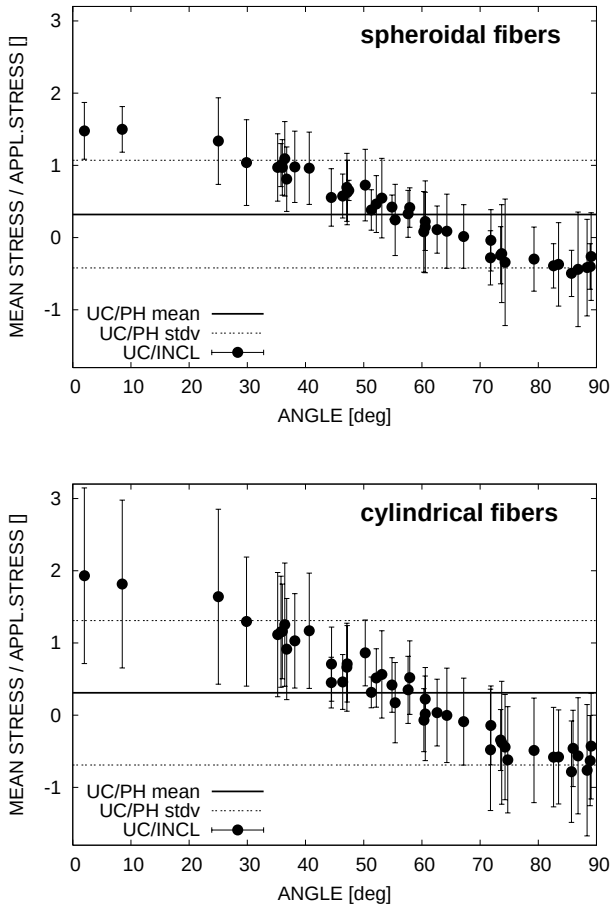

Figure 5 : Normalized mean stresses in the fibers as functions of the angle between the fibers and an applied uniaxial load $\overline{\sigma}$ in the fully yielded regime; results comprise unit cell predictions for an elastoplastic SiC/Al2618 MMC reinforced by randomly oriented spheroidal (top) or cylindrical (bottom) fibers (a=5.0, ξ=0.15, $\overline{\sigma}$=2.45$\sigma_{y,0}^{(m)}$).

figs. 2 and 3, the average stress concentration factors of the fibers are much higher, especially for those nearly aligned with the loading direction. There is a marked tendency for fibers oriented at angles of more than 60° with respect to the loading direction to show compressive mean stresses. In contrast to the elastic case, fig. 3, the fiber shape can be seen to have a marked influence on the average reinforcement stresses, more pronounced inter-fiber variations being predicted for both deviatoric and mean stresses in the cylindrical fibers compared to the spheroidal ones. The intra-fiber fluctuations of the stresses in individual fibers, especially in those subtending small angles to the loading direction, are predicted to be substantial for ellipsoidal reinforcements and very high indeed for cylindrical ones.

The main limitation of the present unit cell approach for modeling the mechanical responses of discontinuously reinforced composites are its high computational costs when nonlinear behaviors are studied. This constitutes a considerable practical obstacle against using unit cells containing high number of fibers or particles and against evaluating a considerable number of different unit cells describing statistically equivalent phase arrangements, both of which are clearly desirable for improving the statistical significance of the results. Finally, it is worth mentioning that both the unit cell approach and the extended Mori–Tanaka method are not limited to the uniaxial loading of randomly oriented fibers, but can be used for any fiber orientation distribution function and for any applied load.

3.2 Particle fracture in composites reinforced by spherical particles

Whereas in section 3.1 three-dimensional multi-inclusion unit cells were used for describing the mechanical behavior of damage-free discontinuously reinforced composites, periodic phase arrangements are now employed for studying a specific damage mode in particle reinforced MMCs, viz. brittle cleavage of the particles. Microscale damage by void nucleation in the matrix or by interfacial decohesion is not accounted for in the model, which is aimed solely at studying particle cracking.

Broadly speaking, there are two strategies for modeling the fracture of particles in MMCs within the framework of continuum micromechanics. One of them deterministically describes the initiation and growth of cracks on the basis of the local stress distributions in the reinforcements, e.g. by employing cohesive zone models, which can be used to follow the progress of cracks in brittle media as well as at the interfaces between elastic and ductile materials, see e.g. Li and Siegmund (2004). Alternatively, the cleavage of particles can be treated as a statistical phenomenon, e.g. by using a probabilistic weakest-link failure criterion such as Weibull-type fracture probabilities that operate at the particle level to trigger cracking along suitably fracture surfaces. Within the present context the main advantage of cohesive zone models lies in their capability for following irregular crack paths,

see e.g. Maiti and Geubelle (2004), whereas the main strength of Weibull-based fracture simulations is their intrinsic sensitivity to the absolute size of the reinforcements, with larger particles being more liable to fail than smaller ones as is typically observed in experiments. Discrete microgeometry analyses using either of the above modeling strategies have been reported in the literature, all of which involved simple phase arrangement or were restricted to planar and axisymmetric microgeometries.

Wallin, Saario, and Törrönen (1987) compared different models for the fracture of brittle particles embedded in a ductile matrix and concluded that weakest-link theories typically give valid predictions for the fraction of broken particles in terms of the particle size and the matrix flow stress. A drawback of using such approaches for modeling the fracture of particles in MMCs is that appropriate populations of flaws have not been identified in typical particles. Simple Weibull-based models also do not correctly predict the dependence of the rate of particle cracking in MMCs on particle size and volume fraction obtained from acoustic emission experiments, compare Mummery, Derby, and Scruby (1993). Accordingly, for studying the brittle failure of particles embedded in a ductile matrix Weibull-based fracture models are best viewed as phenomenological approaches.

Weibull-type concepts have been used by a number of authors for modeling the fracture of particulate reinforcements in MMCs in micromechanical studies employing mean field methods, see e.g. Fitoussi, Bourgeois, Guo, and Baptiste (1995), unit cell models, see e.g. Pandorf (2000) or Ghosh and Moorthy (1998), as well as multiscale approaches, see e.g. Maire, Wilkinson, Embury, and Fougères (1997) and González and LLorca (2000). In most of these models the fracture probabilities were used as Rankine-type criteria, i.e. brittle failure was assumed to take place once the fracture probability in a given particle reached some critical level. In the following, a three-dimensional and fully probabilistic reinforcement fracture model for particle reinforced MMCs is proposed.

Because the original approach of Weibull (1951) was formulated for brittle materials subjected to homogeneous uniaxial stress fields, it must be modified to account for the fact that at the relevant volume fractions some multiaxiality and variability of the stress is always present within the particles in MMCs. A simple two-parameter Weibull-type model for such conditions gives the fracture probability P_k of the k-th particle within a unit cell as

$$P_k = 1 - \exp\left[-\frac{1}{V_0}\int_{V_k:\sigma_1(\mathbf{r})>0}\left(\frac{\sigma_1(\mathbf{r})}{\sigma_\mathrm{f}}\right)^m dV\right] \quad , \qquad (5)$$

where $\sigma_1(\mathbf{r})$ stands for the distribution of the maximum principal stress within the particle as obtained by the micromechanical analysis, $V_k : \sigma_1(\mathbf{r}) > 0$ denotes the region of particle k for which this maximum principal stress is tensile, V_0 is a reference volume that was set equal to the particles' volume for the present study, and m and σ_f are the Weibull modulus and the characteristic strength of the particles, respectively. Equation (5) can be expected to give reasonable results provided the stresses in the particles show only limited multiaxiality, there is no marked variation of the the orientation of the principal stress axes within individual reinforcements, and the inter-particle stress fluctuations are not excessive. The volume integrals were evaluated via eqn. (2) and the Weibull modulus was selected as m=3 for all analyses, which is within the range quoted by LLorca and González (1998). Under such conditions, inter-particle stress fluctuations tend to lead to considerable variations between the fracture probabilities of individual particles, compare Han, Eckschlager, and Böhm (2001).

The fracture probabilities P_k^i of all particles in the unit cell were computed following each load increment in the course of displacement controlled nonlinear Finite Element analyses. Following Pandorf (2000), the probability of failure due to the changes in the stress distributions occurring during increment i within the k-th particle was then evaluated as

$$\Delta P_k^i = \max\left(0, P_k^i - P_k^{\max,i-1}\right) \quad . \qquad (6)$$

Here $P_k^{\max,i-1}$ stands for the maximum value of P_k attained during the previous $i-1$ load steps (note that stress redistribution effects may lead to decreases in the P_k of some particles even as the applied load grows, compare Eckschlager, Böhm, and Han (2002)). For nonzero values of ΔP_k^i a random number was drawn to decide if the increased fracture probability led to failure of the particle. In the case of a positive answer a nodal release technique was employed to split the particle into two parts along a predefined fracture surface, which was taken to pass through the particle center and to be oriented normally to the macroscopic uniaxial stress. The algorithm was implemented via ABAQUS user subroutines; for details see Eckschlager (2002).

The choice of an "instant particle cleavage" model was made for reasons of compatibility with the Weibull concept. The assumption that the orientation of the fracture surfaces is normal to the macroscopic applied stress agrees well with experimental observations of failed particles, see e.g. Mawsouf (2000). The use of fracture surfaces that pass through the inclusion center also appears plausible for spherical reinforcements. The restriction of the present model effort to brittle failure of the particles implicitly introduces an additional assumption, viz. that cracks cannot progress from reinforcements into the matrix or into the interface. This simplification clearly is unrealistic for most actual composites, but was introduced on purpose in order to facilitate the development of algorithms and to allow to study particle cracking in isolation.

Figure 6 shows two deformed states of a 15-particle unit cell obtained by the Weibull-based node release algorithm introduced above, in which two and five particles, respectively, have fractured. Whereas the fractured particles are somewhat difficult to identify at the overall strain of $\bar{\varepsilon}$=0.017 (top), some of the cracks have opened widely at the strain of $\bar{\varepsilon}$=0.144 (bottom). The stress vs. strain diagram obtained from the same simulation run is displayed in fig. 7, the two deformation states depicted in fig. 6 being marked as A and B.

An inspection of fig. 7 shows some features worth discussing. The first two particles can be seen to have failed at relatively low overall stresses, a behavior that is well known from actual ductile matrix composites, and the failure events are fairly unevenly distributed with respect to both macroscopic stresses and strains. The magnitudes of the reductions in the homogenized stress associated with the individual cleavage events are quite high, which is a direct consequence of using a unit cell model with a fairly low number of particles (it may be observed that the failure of one of the 15 particles in the cell corresponds to the simultaneous failure of 6.7% of all particles in the periodic model composite).

Repeating a simulation run with the same unit cell subjected to the same loading conditions in general will lead to different particle failure sequences and different overall stresses at which the failure of a given particle occurs. As an example, fig. 8 shows as thin solid lines three stress vs. strain diagrams obtained with the same unit cell and for the same loading conditions. In contrast to the softest σ–ε-response present (which corresponds to fig. 7) the other two show a rather late onset of particle fracture.

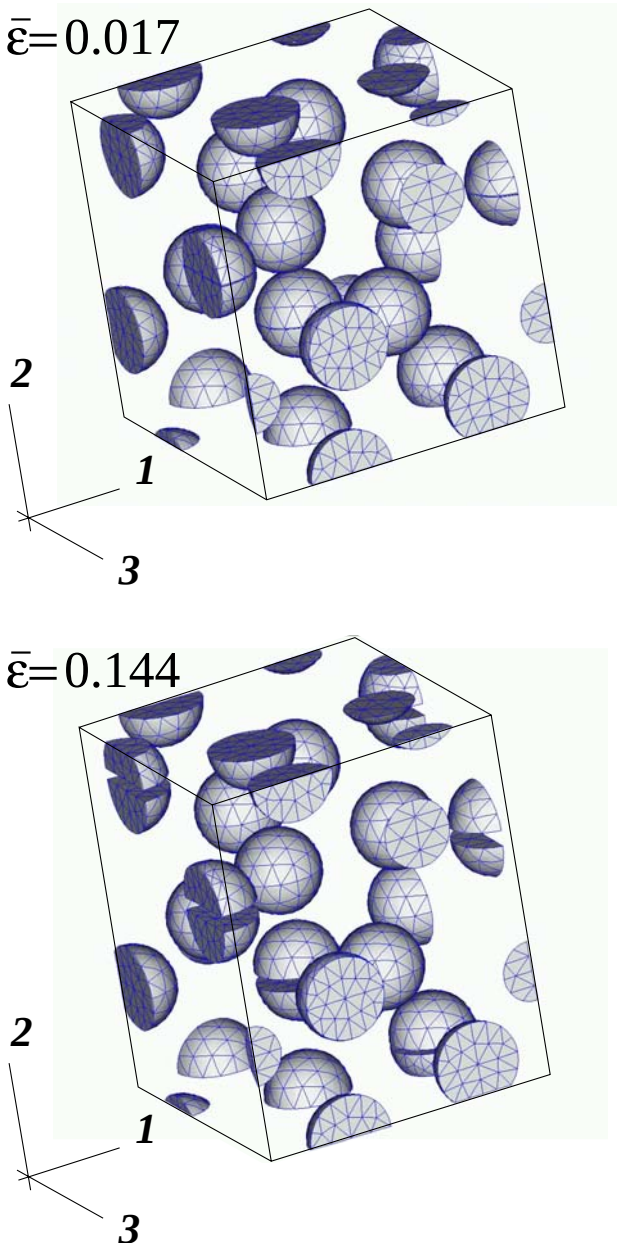

Figure 6 : Deformed configurations of a unit cell for a particle reinforced MMC (ξ=0.15) subjected to uniaxial loading in 2-direction predicted by the Weibull-based particle fracture model; results for macroscopic strains of $\bar{\varepsilon}$=0.017 (2 fractured particles, top) and $\bar{\varepsilon}$=0.144 (5 fractured particles, bottom) are shown.

Such sets of results are best evaluated in terms of their ensemble averaged behavior, which is given in fig. 8 as a bold solid line.

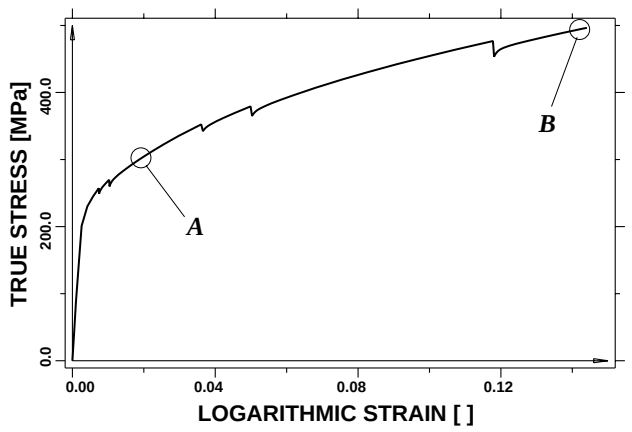

Figure 7 : Stress vs. strain diagram predicted by a unit cell model for a particle reinforced MMC (ξ=0.15) incorporating particle cracking; the states corresponding to the configurations shown in fig. 6 are marked as A and B.

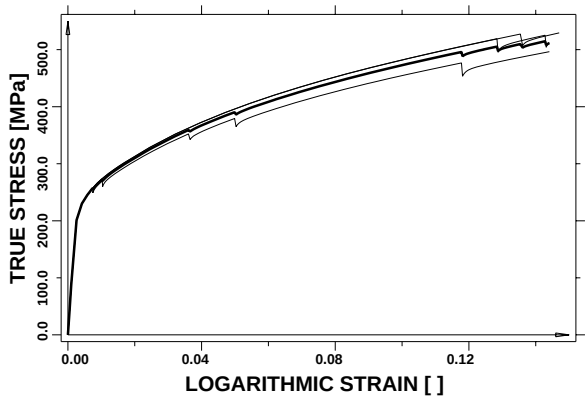

Figure 8 : Stress vs. strain diagrams obtained from three runs using the same unit cell model for a particle reinforced MMC (ξ=0.15) incorporating particle cracking (thin lines); the averaged behavior is shown as a bold solid line.

The present multi-particle unit cell model incorporating particle fracture can handle simulations of multiple consecutive failure of spherical particles on the basis of the realistic stress partitioning provided by a three-dimensional microgeometry. It can be directly used to explore effects of absolute particle size by either changing the size of the unit cell or by modifying the reference volume V_0 in eqn. (5) as well as effects of particle volume fraction and of relative particle size, both of which require the generation of appropriate unit cells.

Considerable work would be required for extending the present model to irregularly shaped particles, for which additional criteria may have to be introduced to define the positions of cracks within each particle, for example on the basis of the local stress fields as proposed by Ghosh and Moorthy (1998). Similar considerations hold for modeling the brittle failure in fiber-like reinforcements, in which multiple cracks may also appear.

4 Conclusions

Three-dimensional multi-inclusion unit cell models were developed and applied successfully for investigating the thermomechanical behavior of ductile matrix composites reinforced by randomly positioned spherical particles or by randomly oriented fibers. In the case of damage-free composites reinforced with randomly oriented fibers excellent agreement with a Mori–Tanaka method was shown in terms of the dependence of the reinforcement microstresses on the fiber orientation. Qualitative differences in the influence of the reinforcement shape on these microstresses were identified between the elastic and fully yielded regimes. For composites subject to brittle failure of the reinforcing particles the Weibull-based probabilistic modeling of consecutive particle cleavage in three-dimensional multi-inclusion unit cells was achieved.

Future developments will, on the one hand, aim at unit cells that contain a higher number of appropriately positioned reinforcements, and further reinforcement shapes will be studied. On the other hand, it is planned to extend the models to account for ductile damage of the matrix as well as for decohesion of the interface between reinforcement and matrix.

References

Agarwal, B.; Broutman, L. (1974): Three-dimensional finite element analysis of spherical particle composites. *Fibre Sci. Technol.*, vol. 7, pp. 63–77.

Agarwal, B.; Panizza, B.; Broutman, L. (1971): Micromechanics analysis of porous and filled ceramic composites. *J. Amer. Ceram. Soc.*, vol. 54, pp. 620–624.

Banerjee, P.; Henry, D. (1992): Elastic analysis of three-dimensional solids with fiber inclusions by BEM. *Int. J. Sol. Struct.*, vol. 29, pp. 2423–2440.

Bao, G. (1992): Damage due to fracture of brittle reinforcements in a ductile matrix. *Acta. metall. mater.*, vol. 40, pp. 2547–2555.

Benveniste, Y. (1987): A new approach to the application of Mori–Tanaka's theory in composite materials. *Mech. Mater.*, vol. 6, pp. 147–157.

Benveniste, Y. (1990): Some remarks on three micromechanical models in composite media. *J. Appl. Mech.*, vol. 57, pp. 474–476.

Berns, H.; Melander, A.; Weichert, D.; Asnafi, N.; Broeckmann, C.; Gross-Weege, A. (1998): A new material for cold forging tools. *Comput. Mater. Sci.*, vol. 11, pp. 166–188.

Böhm, H.; Eckschlager, A.; Han, W. (1999): Modeling of phase arrangement effects in high speed tool steels. In Jeglitsch, F.; Ebner, R.; Leitner, H.(Eds): *Tool Steels in the Next Century*, pp. 147–156, Leoben, Austria. Montanuniversität Leoben.

Böhm, H.; Eckschlager, A.; Han, W. (2002): Multi-inclusion unit cell models for metal matrix composites with randomly oriented discontinuous reinforcements. *Comput. Mater. Sci.*, vol. 25, pp. 42–53.

Böhm, H.; Han, W. (2001): Comparisons between three-dimensional and two-dimensional multi-particle unit cell models for particle reinforced MMCs. *Modell. Simul. Mater. Sci. Engng.*, vol. 9, pp. 47–65.

Christensen, R.; Lo, K. (1979): Solutions for effective shear properties in three phase sphere and cylinder models. *J. Mech. Phys. Sol.*, vol. 27, pp. 315–330.

Christman, T.; Needleman, A.; Suresh, S. (1989): An experimental and numerical study of deformation in metal–ceramic composites. *Acta metall.*, pp. 3029–3050.

Courage, W.; Schreurs, P. (1992): Effective material parameters for composites with randomly oriented short fibers. *Comput. Struct.*, vol. 44, pp. 1179–1185.

Drugan, J.; Willis, J. (1996): A micromechanics-based nonlocal constitutive equation and estimates of representative volume element size for elastic composites. *J. Mech. Phys. Sol.*, vol. 44, pp. 497–524.

Dunn, M.; Ledbetter, H.; Heyliger, P.; Choi, C. (1996): Elastic constants of textured short-fiber composites. *J. Mech. Phys. Sol.*, vol. 44, pp. 1509–1541.

Duschlbauer, D.; Pettermann, H.; Böhm, H. (2003): Mori–Tanaka based evaluation of inclusion stresses in composites with nonaligned reinforcements. *Scr. Mater.*, vol. 48, pp. 223–228.

Eckschlager, A. (2002): *Simulation of Particle Failure in Particle Reinforced Ductile Matrix Composites*. PhD thesis, Vienna University of Technology, Vienna, Austria, 2002.

Eckschlager, A.; Böhm, H.; Han, W. (2002): A unit cell model for brittle fracture of particles embedded in a ductile matrix. *Comput. Mater. Sci.*, vol. 25, pp. 75–91.

Eshelby, J. (1957): The determination of the elastic field of an ellipsoidal inclusion and related problems. *Proc. Roy. Soc. London*, vol. A241, pp. 376–396.

Ferrari, M. (1991): Asymmetry and the high concentration limit of the Mori–Tanaka effective medium theory. *Mech. Mater.*, vol. 11, pp. 251–256.

Fitoussi, J.; Bourgeois, J.; Guo, G.; Baptiste, D. (1995): Prediction of the anisotropic damaged behavior of composite materials: Introduction of multilocal failure criteria in a micro–macro relationship. *Comput. Mater. Sci.*, vol. 5, pp. 87–100.

Fond, C.; Riccardi, A.; Schirrer, R.; Montheillet, F. (2001): Mechanical interaction between spherical inhomogeneities: An assessment of a method based on the equivalent inclusion. *Eur. J. Mech. A/Solids*, vol. 20, pp. 59–75.

Ghosh, S.; Moorthy, S. (1998): Particle fracture simulation in non-uniform microstructures of metal-matrix composites. *Acta mater.*, vol. 46, pp. 965–982.

González, C.; LLorca, J. (2000): A self-consistent approach to the elasto-plastic behavior of two-phase materials including damage. *J. Mech. Phys. Sol.*, vol. 48, pp. 675–692.

Gusev, A. (1997): Representative volume element size for elastic composites: A numerical study. *J. Mech. Phys. Sol.*, vol. 45, pp. 299–307.

Gusev, A.; Hine, P.; Ward, I. (2000): Fiber packing and elastic properties of a transversely random unidirectional glass/epoxy composite. *Compos. Sci. Technol.*, vol. 60, pp. 535–541.

Gusev, A.; Lusti, H.; Hine, P. (2002): Stiffness and thermal expansion of short fiber composites with fully aligned fibers. *Adv. Engng. Mater.*, vol. 4, pp. 927–931.

Han, W.; Eckschlager, A.; Böhm, H. (2001): The effects of three-dimensional multi-particle arrangements on the mechanical behavior and damage initiation of particle-reinforced MMCs. *Compos. Sci. Technol.*, vol. 61, pp. 1581–1590.

Hashin, Z. (1983): Analysis of composite materials — A survey. *J. Appl. Mech.*, vol. 50, pp. 481–505.

Hashin, Z.; Shtrikman, S. (1962): On some variational principles in anisotropic and nonhomogeneous elasticity. *J. Mech. Phys. Sol.*, vol. 10, pp. 335–342.

Huet, C.; Navi, P.; Roelfstra, P. (1991): A homogenization technique based on Hill's modification theorem. In Maugin, G.(Ed): *Continuum Models and Discrete Systems*, pp. 135–143, Harlow, UK. Longman.

Ingber, M.; Papathanasiou, T. (1997): A parallel-supercomputing investigation of the stiffness of aligned short-fiber-reinforced composites using the boundary element method. *Int. J. Num. Meth. Engng.*, vol. 40, pp. 3477–3491.

Ingber, M.; Womble, D.; Mondy, L. (1992): A parallel boundary element formulation for determining effective properties of heterogeneous media. *Int. J. Num. Meth. Engng.*, vol. 37, pp. 3905–3919.

Jiang, M.; Ostoja-Starzewski, M.; Jasiuk, I. (2000): Bounding of effective elastoplastic response of random composite. In Khan, A.; Zhang, H.; Yuan, Y.(Eds): *Plastic and Viscoplastic Response of Materials and Metal Forming*, pp. 528–530, Fulton, MD. NEAT Press.

Lee, K.; Moorthy, S.; Ghosh, S. (1999): Multiple scale computational model for damage in composite materials. *Comput. Meth. Appl. Mech. Engng.*, vol. 172, pp. 175–201.

Levy, A.; Papazian, J. (1990): Tensile properties of short fiber-reinforced SiC/Al composites: Part II. Finite element analysis. *Metall. Trans.*, vol. 21A, pp. 411–420.

Li, W.; Siegmund, T. (2004): Numerical study of indentation delamination of strongly bonded films by use of a cohesive zone model. *CMES: Computer Modeling in Engineering & Sciences*. Volume 5, No. 1, pp. 81–90.

LLorca, J.; González, C. (1998): Microstructural factors controlling the strength and ductility of particle reinforced metal-matrix composites. *J. Mech. Phys. Sol.*, vol. 46, pp. 1–28.

LLorca, J.; Martín, A.; Ruiz, J.; Elices, M. (1993): Particulate fracture during deformation of a spray formed metal-matrix composite. *Metall. Trans.*, vol. 24A, pp. 1575–1588.

Lusti, H.; Hine, P.; Gusev, A. (2002): Direct numerical predictions for the elastic and thermoelastic properties of short fibre composites. *Compos. Sci. Technol.*, vol. 62, pp. 1927–1934.

Maire, E.; Wilkinson, D.; Embury, J.; Fougères, R. (1997): Role of damage on the flow and fracture of particulate reinforced alloys and metal matrix composites. *Acta mater.*, vol. 45, pp. 5261–5274.

Maiti, S.; Geubelle, P. (2004): Mesoscale modeling of dynamic fracture of ceramic materials. *CMES: Computer Modeling in Engineering & Sciences*. Volume 5, No. 2, pp. 91–101.

Mawsouf, N. (2000): A micromechanical mechanism of fracture initiation in discontinuously reinforced metal matrix composite. *Mater. Charact.*, vol. 44, pp. 321–327.

Michel, J.; Moulinec, H.; Suquet, P. (1999): Effective properties of composite materials with periodic microstructure: A computational approach. *Comput. Meth. Appl. Mech. Engng.*, vol. 172, pp. 109–143.

Michel, J.; Moulinec, H.; Suquet, P. (2000): A computational method based on augmented Lagrangians and fast Fourier transforms for composites with high contrast. *CMES: Computer Modeling in Engineering & Sciences*, vol. 1, pp. 79–88.

Mishnaevsky, L.; Lippmann, N.; Schmauder, S. (2001): Computational modeling of crack propagation in real and artificial microstructures of tool steels. In Schmauder, S.; Mishnaevsky, L.(Eds): *Damage in Metallic Multiphase Materials: Mechanisms and Mesomechanics*. MPA Stuttgart, Stuttgart.

Mlekusch, B. (1998): Thermoelastic properties of short-fibre-reinforced thermoplastics. *Compos. Sci. Technol.*, vol. 59, pp. 911–923.

Mummery, P.; Derby, B.; Scruby, C. (1993): Acoustic emission from particulate-reinforced metal matrix composites. *Acta metall. mater.*, vol. 41, pp. 1431–1445.

Ostoja-Starzewski, M. (1998): Random field models of heterogeneous materials. *Int. J. Sol. Struct.*, vol. 35, pp. 2429–2455.

Pandorf, R. (2000): *Ein Beitrag zur FE-Simulation des Kriechens partikelverstärkter metallischer Werkstoffe*. VDI–Verlag, Düsseldorf.

Pettermann, H.; Böhm, H.; Rammerstorfer, F. (1997): Some direction dependent properties of matrix–inclusion type composites with given reinforcement orientation distributions. *Composites*, vol. 28B, pp. 253–265.

Ponte Castañeda, P.; Suquet, P. (1998): Nonlinear composites. In van der Giessen, E.; Wu, T.(Eds): *Advances in Applied Mechanics 34*, pp. 171–302, New York, NY. Academic Press.

Ponte Castañeda, P.; Willis, J. (1995): The effect of spatial distribution on the effective behavior of composite materials and cracked media. *J. Mech. Phys. Sol.*, vol. 43, pp. 1919–1951.

Rintoul, M.; Torquato, S. (1997): Reconstruction of the structure of dispersions. *J. Colloid Interf. Sci.*, vol. 186, pp. 467–476.

Schjødt-Thomsen, J.; Pyrz, R. (2001): The Mori–Tanaka stiffness tensor: Diagonal symmetry, complex fibre orientations and non-dilute volume fractions. *Mech. Mater.*, vol. 33, pp. 531–544.

Segurado, J.; LLorca, J. (2002): A numerical approximation to the elastic properties of sphere-reinforced composites. *J. Mech. Phys. Sol.*, vol. 50, pp. 2107–2121.

Segurado, J.; LLorca, J.; González, C. (2002): On the accuracy of mean field approaches to simulate the plastic deformation of composites. *Scr. mater.*, vol. 46, pp. 525–529.

Shen, H.; Lissenden, C. (2002): 3D finite element analysis of particle-reinforced aluminum. *Mater. Sci. Engng.*, vol. A338, pp. 271–281.

Sørensen, N.; Suresh, S.; Tvergaard, V.; Needleman, A. (1995): Effects of reinforcement orientation on the tensile response of metal matrix composites. *Mater. Sci. Engng.*, vol. A197, pp. 1–10,.

Suquet, P. (1987): Elements of homogenization for inelastic solid mechanics. In Sanchez-Palencia, E.; Zaoui, A.(Eds): *Homogenization Techniques in Composite Media*. Springer–Verlag, Berlin.

Suquet, P. (1995): Overall properties of nonlinear composites: A modified secant moduli theory and its link with Ponte Castañeda's nonlinear variational procedure. *C. R. Acad. Sci. Paris, série IIb*, vol. 320, pp. 563–571.

Torquato, S. (1991): Random heterogeneous media: Microstructure and improved bounds on effective properties. *Appl. Mech. Rev.*, vol. 44, pp. 37–75.

Tvergaard, V. (1990): Analysis of tensile properties for a whisker-reinforced metal-matrix composite. *Acta metall. mater.*, vol. 38, pp. 185–194.

Tvergaard, V. (1993): Model studies of fibre breakage and debonding in a metal reinforced by short fibres. *J. Mech. Phys. Sol.*, vol. 41, pp. 1309–1326.

Wallin, K.; Saario, T.; Törrönen, K. (1987): Fracture of brittle particles in a ductile matrix. *Int. J. Fract.*, vol. 32, pp. 201–209.

Weibull, W. (1951): A statistical distribution function of wide applicability. *J. Appl. Mech.*, vol. 18, pp. 293–297.

Weissenbek, E.; Böhm, H.; Rammerstorfer, F. (1994): Micromechanical investigations of arrangement effects in particle reinforced metal matrix composites. *Comput. Mater. Sci.*, vol. 3, pp. 263–278.

Yotte, S; Riss, J; Breysse, D; Ghosh, S. (2004): Cluster Analysis for Particle Reinforced Metal Matrix Composites, *CMES: Computer Modeling in Engineering & Sciences*. Volume 5, No. 2, pp. 171–187.

Zeman, J.; Šejnoha, M. (2001): Numerical evaluation of effective elastic properties of graphite fiber tow impregnated by polymer matrix. *J. Mech. Phys. Sol.*, vol. 49, pp. 69–90.

Zohdi, T.; Wriggers, P. (2001): A model for simulating the deterioration of structural-scale material responses of microheterogeneous solids. *Comput. Meth. Appl. Mech. Engng.*, vol. 190, pp. 2803–2823.